

# The Effects of Degradation Phenomena of the Steel-Concrete Interface in Reinforced Concrete Structures

Bozabe Renonet Karka<sup>1\*</sup>, Bassa Bruno<sup>2</sup>, Nadjitonon Ngarmaim<sup>3</sup>, Alladjo Rimbarngaye<sup>4</sup>

<sup>1</sup>Department of Civil Engineering, National High School of Public Works (NHSPW), University of N'Djamena, N'Djamena, Chad

<sup>2</sup>Laboratory of Studies and Realization in Industrial Techniques (LSRIT), Faculty of Exact and Applied Sciences (FEAS), University of N'Djamena, N'Djamena, Chad

<sup>3</sup>Department of Technology, Faculty of Exact and Applied Sciences (FEAS), University of N'Djamena, N'Djamena, Chad

<sup>4</sup>Department of Civil and Construction Engineering, Pan African University Institute for Basic Sciences, Technology and Innovation hosted at Jomo Kenyatta University of Agriculture and Technology, Juja, Kenya

Email: \*enstp2020@gmail.com

**How to cite this paper:** Karka, B.R., Bruno, B., Ngarmaim, N. and Rimbarngaye, A. (2023) The Effects of Degradation Phenomena of the Steel-Concrete Interface in Reinforced Concrete Structures. *Journal of Materials Science and Chemical Engineering*, 11, 1-21.

<https://doi.org/10.4236/msce.2023.113001>

**Received:** November 10, 2022

**Accepted:** March 20, 2023

**Published:** March 23, 2023

Copyright © 2023 by author(s) and Scientific Research Publishing Inc.

This work is licensed under the Creative Commons Attribution International License (CC BY 4.0).

<http://creativecommons.org/licenses/by/4.0/>



Open Access

## Abstract

Reinforced concrete (RC) constructions are the innovation of sustainable constructions replacing masonry constructions. Despite this, the use of concrete and steel to improve the performance of structural members in service is a recurring problem due to the immediate or overtime appearance of cracks. The objective of this work was therefore to assess the damage phenomena of the steel-concrete interface in order to assess the performance of an RC structure. Samples of approximately 30 cm of reinforcement attacked by rust were taken from broken reinforced concrete columns and beams in order to determine the impact of corrosion on high adhesion steel (HA) and therefore on its ability to resist. The experimental results have shown that the corrosion degradation rates of reinforcing bars of different diameters increase as the diameter of the reinforcing bars decreases: 5% for HA12; 23.75% for HA8 and 50% for HA6. Using the approach proposed by Mangat and Elgalf on the bearing capacity as a function of the progress of the corrosion phenomenon, these rates made it possible to assess the new fracture limits of corroded HA steels. For HA6 respectively HA8 and HA12, their initial limit resistances will decrease by 4/4, 3/4 and 1/4. Based on the results of this study and in order to guarantee their durability, an RC structure can be dimensioned by taking into account the effects of reinforcement corrosion.

## Keywords

Reinforced Concrete Construction, Steel-Concrete Interface, Corrosion Degradation Rate, Adhesion, Bearing Capacity

## 1. Introduction

Concrete in general, a material with a strong tendency to crack is widely used throughout the world for so-called durable constructions. In reinforced concrete structures, cracks develop particularly in areas subject to bending-type stresses (traction-compression) [1]. Also, some infrastructure soils lend themselves well to this.

Indeed, concrete resists compression well, but, in traction, it has an almost fragile behaviour and low resistance (10 times lower than that measured in compression). This is why it is associated with steel [2]. While steel reinforcements provide good mechanical strength, they do not completely prevent the appearance of cracks in concrete [3].

Concrete cracking is characterized by the appearance of micro-cracks that can appear in the material as soon as it is installed (consequence of the phenomenon of shrinkage at a young age, for example). These micro-cracks then propagate in the structure as it is stressed. Under the effect of greater stresses, macro cracks develop and can cause the structure to collapse [4].

Technicians and engineers in the civil engineering profession have always wondered whether the types of soil subject to tension-compression stresses are solely responsible for cracks in concrete. This question led them to examine the steel-concrete interfaces to determine if they are not also probable sources of cracking.

Numerous studies carried out by researchers have indeed shown that in the steel-concrete interfaces, complex phenomena can arise, which will lead to the ruin of the structure [5]-[13]. It is now a question of seeking to particularly locate the responsibilities of these degradation phenomena of the steel-concrete interface and the consequences in order to substantially reduce the damage that appears immediately or over time in reinforced concrete structures.

## 2. Literature Review

The various degradation phenomena of the steel-concrete interface are, among others the loss of adhesion between steel and concrete and the phenomenon of corrosion of the reinforcements in the concrete [14].

### 2.1. Loss of Adhesion

Reinforced concrete is the result of the combination of two materials, concrete and steel. These materials have complementary properties. One resists both traction and compression while the other resists compression well but its tensile strength is low, which makes this type of concrete very strong [15]. This property in particular explains its success in the construction industry. But, the effectiveness of this association would be nothing without one particular phenomenon: the bond between steel and concrete.

When designing a reinforced concrete element, it is considered that the adhesion between the concrete and the steel is perfect because it allows, among other

things, the reinforcements not to slip in the concrete. In fact, during loading, the rebars are able to slide inside the element. This is a phenomenon attributed to the difference between the elastic E module of the two materials [16]. Other aspects of mix design and concrete placement techniques can also be responsible for excessive slippage if the cover quality of the rebar is compromised [17].

The steel-concrete bond corresponds to a physical interaction between these two different materials, the purpose of which is to ensure the transfer and continuity of forces and stresses in their contact zone [18]. It is governed by three main mechanisms: chemical adhesion, friction and rib/concrete interaction. Adhesion can be favoured or unfavourable by the difference between the Young E's module of the two materials, the quality of the cover concrete, the workmanship and the surface condition of the steel [19].

Young's modulus E, according to its definition, is the ratio of the axial stress to the corresponding unit linear strain: This is Hooke's law which is written:

$$E = \sigma / \varepsilon \quad (1)$$

with,  $\sigma$ : axial stress and  $\varepsilon$ : unit linear strain.

E has the dimensions of a stress in MPa and is between 2.104 and 4.104 MPa for concrete and 2.105 and 2.1.105 MPa for steel.

Degradation of the bond through slippage of the reinforcement generally involves cylindrical cracking. This must pass through one and/or the other of the two materials. Concrete has a lower Young's modulus in compression than steel, which is an order of magnitude stiffer and stronger than concrete. This difference in modulus will have a negative influence on the bond, because these two materials (steel and concrete) do not have the same capacity to deform together as a single material [20]. Thus, bond degradation occurs only in concrete near steel.

The coating must be sufficient to guarantee good transmission of adhesion forces, good protection of the steel and suitable fire resistance.

The quality of the cover concrete is conditioned by the dosage and the vibration conditions which influence the compactness. The formulation and preparation of concrete, the methods of placing and curing must allow the concrete to develop all its qualities [21].

Bars with surfaces showing irregularities or roughness (roughness, relief) are characterized by very high adhesion (2 to 3 times greater than that of smooth round steels (RL)). They achieve 70% to 75% of the total bond strength [22]. Equation (3) allowed us to calculate the bond stress noted  $\tau_{su}$ . In **Table 1**, we have presented a comparative example of the bond stresses of HA and RL steels for a compressive strength of concrete at 28 days equal to 25 MPa.

**Table 1.** Comparison of bond stresses  $\tau_{su}$  between HA and RL steels.

Steels	$f_{c28}$ in MPa	$\Psi_s$	$\tau_{su}$ in MPa
HA	2.10	1.50	2.84
RL	2.10	1.00	1.26

In addition, it should be remembered that  $\tau_{su}$  due to shrinkage deformations generally presents 10% to 15% of the total adhesion resistance. As for  $\tau_{su}$  due to the bonding of cement to steel, it is of the order of 0.2 to 0.5 MPa [23].

## 2.2. The Corrosion Phenomenon

In the case of reinforced concrete structures, the resistance of steels to corrosion is the main factor to be taken into account when studying the durability of different types of structures. Corrosion of reinforcements is the cause of about 80% of the degradation of these types of structures and works [24]. Their lifespan is conditioned by the response to physical and chemical attacks from the environment, as well as by the ability of the constituent materials to protect themselves against these attacks [25]. To this end, it is very important to know the corrosion process and its environmental and structural interactions.

Corrosion will develop mainly according to two processes: slow and uniform carbonation of the concrete along the reinforcement and attack by chlorides which, when they are in sufficient quantity around the reinforcement, generate pitting of corrosion [26]. This process is rapid in terms of kinetics and highly localized. When corrosion becomes active, the mechanical behaviour of the structure changes. This is mainly due to the reduction in the section of corroded reinforcement which can lead to a reduction in the mechanical resistance thereof. The volume of corroded steel is significantly greater than that of sound steel. This volumetric increase generates pressure on the concrete and thus cracks or bursting of the cover concrete [27] [28] [29] [30]. Over the past two decades, much research has been done on the corrosion of reinforcement in concrete with the aim of predicting its influence [31] [32] [33] [34] [35]. The effects and consequences of corrosion are diverse and can be represented by the diagram in Figure 1 [36].

The causes of corrosion are multiple and complex and they result from chemical

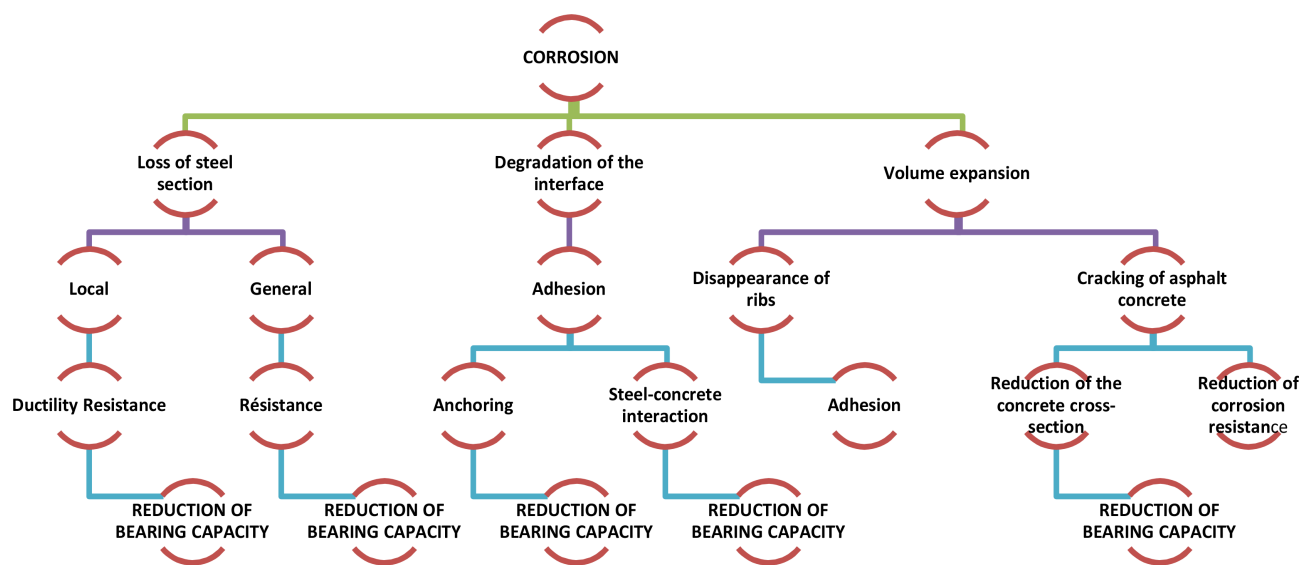


Figure 1. Effects of corrosion on the mechanical behaviour of corroded structures.

and/or physical interactions between the material and its environment. Corrosion phenomena therefore depend on the material and the surrounding environment.

The different parameters that promote the corrosion of a material are: Chemical composition and microstructure of the metal, chemical composition of the environment, physical parameters (temperature, irradiation, etc.) and mechanical stresses (stresses, shocks, friction, etc.) [37].

The different types of corrosion are: Chemical corrosion; biochemical corrosion and electrochemical corrosion [38] [39]. As a general rule, it is considered that corrosion can only take place when aggressive agents have penetrated the cover concrete and reached the reinforcement.

### 3. Material and Methods

#### 3.1. Material

We give a brief overview of the materials used for this study. These are ordinary concrete used in the construction of buildings and general works with a density varying between 2.0 and 2.5 t/m<sup>3</sup>, high adhesion steel (HA) and steel-concrete interface.

##### 3.1.1. Concrete

Concrete, the physical properties of which are given in **Table 2** below, is an artificial stone obtained from a correctly dosed mixture (that is to say in well-determined proportions) of binder, water, aggregates (large and small) and possibly additives. This mixture, when wet, is called fresh concrete. After hydration, it hardens to give a very resistant stone called concrete. It is mainly used for its resistance in compression.

According to **Table 3** below, in a volume of concrete, the different components are in different proportions.

The characteristic strengths of concrete are: compressive strength  $f_{c28}$  (main characteristic determined by a standardized laboratory test); the tensile strength

**Table 2.** Physical properties of concrete.

Density	0.4 to 5.0 t/m <sup>3</sup>
Impermeability	Non
Softening coefficient	Kram $\geq$ 0.8
Thermal conductivity	0.1 to 2.0 W/m °C
Thermal expansion coefficient	$7 \times 10^{-6} \text{ } ^\circ\text{C}^{-1}$ to $15 \times 10^{-6} \text{ } ^\circ\text{C}^{-1}$

**Table 3.** Proportions of the different components of concrete.

Constituents	Binder	Water	Aggregates	Admixture	Air
Absolute volume in %	6 - 15	18 - 30	60 - 80	0 - 1	1 - 6
Weight in %	7 - 15	3 - 12	75 - 85	0 - 1	-

$f_{c28}$  and the shear (sliding) strength  $\tau_{bj}$ ,

During its hardening, the concrete takes, little by little, its resistance and at the end of the 28<sup>th</sup> day, this resistance reaches its characteristic value, designating the class of concrete. The resistance of concrete increases according to a logarithmic law of formula (2) below:

$$f_{cj} = \frac{\log(j)}{\log(7)} \cdot f_{c28} \cong 0.685 f_{c28} \cdot \log(j+1) \quad (2)$$

where,  $j$  is the age of the concrete, in days ( $d \leq 28$  days) and  $f_{c28}$  is the strength of the concrete at 28 days of age, expressed in MPa.

The characteristic compressive strength of concrete at age “ $j$ ”, when “ $j$ ” is very large, can be determined by the following formula (3):

$$f_{cj} = 1.1 f_{c28} \quad \text{for } j > 28 \quad (3)$$

The tensile strength of concrete ( $f_{tj}$ ) is determined by relation (4) below:

$$f_{tj} = 0.6 + 0.06 f_{c28} \quad (4)$$

For calculations in RC, the tensile strength of concrete is neglected.

The shear strength  $\tau_{bj}$  is calculated by formula (5) below:

$$\tau_{bj} = k_c \cdot f_{tj} \quad (5)$$

where,  $k_c = (1.5 - 2.0)$  is a coefficient depending on the class of the concrete.

The deformations of concrete are: shrinkage (of the order of  $5 \times 10^{-4}$ ), swelling (often neglected) and creep.

### 3.1.2. Steel

Considered as a reinforcing element, steel is an alloy of iron (approximately 98%) and carbon (up to 2.0%) containing a very low percentage of impurities (originating from mining or formed during manufacturing) as well as adjuvant (up to 10% sometimes) to improve its qualities [40].

The steels used in reinforced concrete structures are: smooth rounds (RL, in French), which have no roughness on the surface and high adhesion steels (HA), having roughness to improve the steel-concrete adhesion. Concrete steels have different grades which correspond to their qualities of elasticity limit (varies between 200 and 500 MPa) and resistance [41].

The density of steel is  $7.85 \text{ t/m}^3$  (2 to 3 times greater than that of concrete). Thanks to its high mechanical resistance, it is considered the lightest construction material (2 times lighter than wood and 10 times lighter than ordinary concrete). Its coefficient of thermal conductivity is  $58.35 \text{ W/m} \cdot ^\circ\text{C}$  (40 times that of concrete). At  $200^\circ\text{C}$ , its modulus of elasticity  $E$  decreases and at  $600^\circ\text{C}$  already, it changes to the plastic state [42].

The main mechanical characteristics of steel are its mechanical resistance and its deformability, which depend on its composition and the technology of its manufacture. The strain diagrams of steel in tension and in compression are identical; they are symmetrical with respect to the origin O. These diagrams make it possible to determine the mechanical characteristics of steels (the elastic

limit  $F_e$  and the resistance limit  $F_{rup}$ ), the characteristic unit strains of elasticity  $\varepsilon_{el}$ , of rupture  $\varepsilon_{rup}$  and the modulus of elasticity  $E$  [43].

### 3.1.3. Steel-Concrete Interface

In general, a load-bearing reinforced concrete element is a complex system made up of several components (concrete, steel, and interface) whose behaviours are very different from each other. The behaviour of the structure depends essentially not only on the behaviour of concrete and steel but also on that of the steel-concrete interface.

By definition, the interface can be considered to be an area of concrete that surrounds the steel, and which does not a priori have any specified shape. Its shape depends directly on that of steel. The behaviour of the interface is represented by the adhesion which is a complex phenomenon and makes it possible to ensure a bond between two surfaces in contact and to transmit a stress exerted according to the contact surface of the two materials.

In the sense of reinforced concrete, once the concrete is subjected to external loads, the loading of the reinforcements is necessary for the normal functioning of the structure. Thus, this role is performed by the interface. The latter must allow total transmission of forces without slipping of the reinforcements in the concrete sheath before its deterioration. Once the deterioration of the interface has taken place, it causes a loss of adhesion which then leads to a change in the behaviour of steel and concrete [44]. It is therefore necessary to have a good understanding of the behaviour of the interface during structural calculations and during the execution of the work.

The investigation of the behaviour of the interface presented by Lutz and Gergely made it possible to conclude that the transmission of the force between the concrete and the steel takes place by the action of the following three physical phenomena: A physicochemical adhesion, directly linked to the composition of each of them and the way they are set up; a mechanical interaction, this mechanical action is particularly due to the presence of ribs along the reinforcing RCr and friction between the two contact surfaces [45]. These physical phenomena depend on various parameters: the dimensions of the structure, the nature of concrete, reinforcement and its characteristics [46].

For ribbed steels, mechanical interaction is the main mechanism governing the behaviour of the interface. On the contrary, physic-chemical adhesion and friction are the mechanisms which dominate the behaviour of the interface in the case of smooth steels [47] [48] [49] [50]. Under the action of these physical phenomena and according to Caquot's theory, two types of stresses can develop at the interface: Shear stresses generated by sliding along the axis of the RCr. If the axial force increases, these stresses can cause the concrete to break along conical surfaces inclined at an angle of  $45^\circ$  with the axis of the RCr and radial stresses perpendicular to the axis of the RCr (Perchat [51], Tefers [52], Tilantera and Rechart [53]). The essential value characterizing the steel-concrete bond is its shear strength. This data makes it possible to determine the resistance

of a steel cast in concrete, as well as to define an anchoring length necessary to maintain the link. The ultimate adhesion stress  $f_{bd}$ , also called  $\tau_{max}$  in work relating to adhesion (Equation (5)), is calculated experimentally according to the following expression:

$$\tau_{max} = F_{max} / (\pi \cdot \varnothing \cdot l_b) \quad (6)$$

with,  $F_{max}$ : maximum force obtained experimentally;  $\varnothing$ : diameter of the steel;  $l_b$ : length anchored in the concrete.

The regulatory ultimate limit value of the adhesion stress is noted  $\tau_{su}$  and is valid according to the BAEL 91 rules:

$$\tau_{su} = 0.6 \cdot \varphi_s \cdot f_{tj} \quad (7)$$

$\varphi_s$ : The sealing coefficient relating to steel (equal to 1.5 for HA and 1 for RL).

For HA reinforcements, the calculation value of the ultimate bond strength  $f_{bd}$  can be taken according to Eurocode 2, part 8.4.2 equal to:

$$f_{bd} = 2.25 \cdot n_1 \cdot n_2 \cdot f_{ctd} \quad (8)$$

with,  $n_1$  is a coefficient linked to the conditions of adhesion:  $n_1 = 1$ , when the conditions of adhesion are "good" and  $n_1 = 0.7$  in the other cases;  $n_2$  is a coefficient linked to the diameter of the RCr and is equal to the max  $((1.32 - \varphi)/100; 1)$ ;  $f_{ctd}$ : the design tensile strength of concrete as indicated in EC2 in part 3.1.6 [54].

As a reminder, the tests which make it possible to study the behaviour of the steel-concrete interface are: The pull-out type test or pull-out test, the push-in type test and the double tie rod [55].

The intrinsic behaviour of the interface at the local level is influenced by various external factors and parameters (limiting conditions, loads, sizing) and/or internal parameters (characteristics of materials: concrete, steel, adhesion). These parameters can occur at several scales and at different stages of interface degradation.

According to several documentary studies, the main parameters that influence the behaviour of the interface are: The geometrical characteristics of the steel, the characteristics of the concrete, the type of loading and the confinement. Other so-called secondary parameters are: Concrete placement, corrosion and age of concrete [56] [57] [58] [59] [60].

When we talk about the cracking of reinforced concrete, we must necessarily talk about the degradation of the steel-concrete bond, since this one produces radial micro-cracks which can evolve towards different failure mechanisms, and in certain cases, they will be able to cause the fall of the resistance of the integrated system of the three components: steel-bond-concrete. Depending on these three components, failure can occur: either in concrete (longitudinal cracks), or in steel (plasticization of the reinforcement), or in the connection (cylindrical cracks) [61].

### 3.2. Methods

Some accidents in reinforced concrete structures have unexplained causes when

you can be sure that they do not come from the constituents and composition of the concrete, nor from the quality of the steel and the bearing capacity of the sub-floors.

Degradation in the steel-concrete interfaces is one explanatory approach. Experimentally, the type of degradation by corrosion of these interfaces, the consequences of which are on the one hand the initiation and propagation of cracks in the concrete by swelling of the rust and on the other hand, the weakening of the limit to the rupture of reinforcements by reduction of the sections of corroded high-adhesion steels. In this part of the study, we present a method for evaluating the rate of degradation of the steel-concrete interface by corrosion to assess the bearing capacity of a structural element.

### 3.2.1. Study Samples

To show the corrosion degradation of High Adhesion (HA) steel reinforcements, we cut out pieces of steel of about 30 cm that were attacked by rust. They were taken from reinforced concrete posts and beams intended for waste reception or recycling (**Figure 2**). The diameters of these uncorroded samples are respectively, from left to right, 6 mm, 8 mm and 12 mm (**Figure 3**).



**Figure 2.** Samples of the reinforcements taken showing a layer of rust.



**Figure 3.** Standard uncorroded reinforcements in HA steel.

### 3.2.2. Work Equipment

The study was conducted at the Civil Engineering Laboratory of the National High School of Public Works (NHSPW) in N'Djamena, Chad. The latitude, longitude and altitude are respectively 12.132965; 15.0540224 and 298 meters. According to the Google Maps application, consulted on April 25, 2018 at 10:00 a.m., the coordinates of the site are: 12°07'58.7"N 15°03'14.5"E.

Samples should be cleaned using the drill hammer, half-round, medium-sized file and wire brush. Indeed, the hacksaw is used to cut steels into pieces of about 30 cm each; the pitting hammer removes the surface layer of rust; the medium-soft file is used to remove the resistant layer of rust; the wire brush, to clean the sample and the calliper, to measure the diameter of steels with the surface layer of rust and without this layer.

### 3.2.3. Work Performed

#### 1) Sample collection

For our work, we took samples from all sources, the origin and age of which we do not know, since they were taken from broken load-bearing structures intended for the recycling center. The objective here is to determine the impact of corrosion on steel and therefore on its ability to resist, the rate of reduction of which could be assessed.

#### 2) Measurement of the rough rusty section

The samples being well cleaned, it is a question of measuring the new diameters of the parts most affected by corrosion using the calliper. You will first need to know how to read the measurements made with a calliper. The reading example is given below.

Vernier scale  $1/10^{\text{th}}$

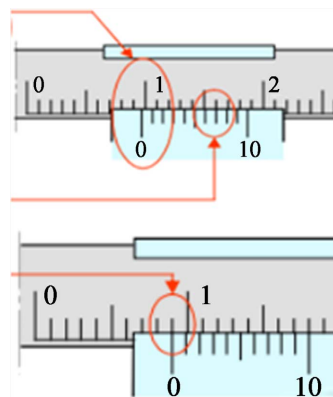
a) The zero of the vernier is opposite a graduation of the ruler.

Read on the ruler the number of mm before the zero of the vernier; here 9 mm.

b) The zero of the vernier is not opposite a graduation of the ruler.

Locate the vernier scale, tenths of an mm, which is best aligned, here 0.60 mm.

We finally read:  $9 + 0.60 = 9.60$  mm.



#### 3) Removal of the rust layer

With the pitting hammer, we had to tap on the rusty sample to remove all the

rusty layer, then we filed down the resistant layers of the rust with the medium-soft file and finally we used the wire brush to clean sample. Thus, we have samples of which the parts most affected by corrosion are revealed to be measured with the calliper.

#### 4) Measurement of the net section most affected by rust

Using the caliper, the most damaged (degraded) sections are measured, as it is this section that is considered to be the least resistant part during a bending force of the structure, for example. These operations are presented in **Figure 4** for HA6, **Figure 5** for HA8 and **Figure 6** for HA 12. All measured values are grouped in **Table 4**.

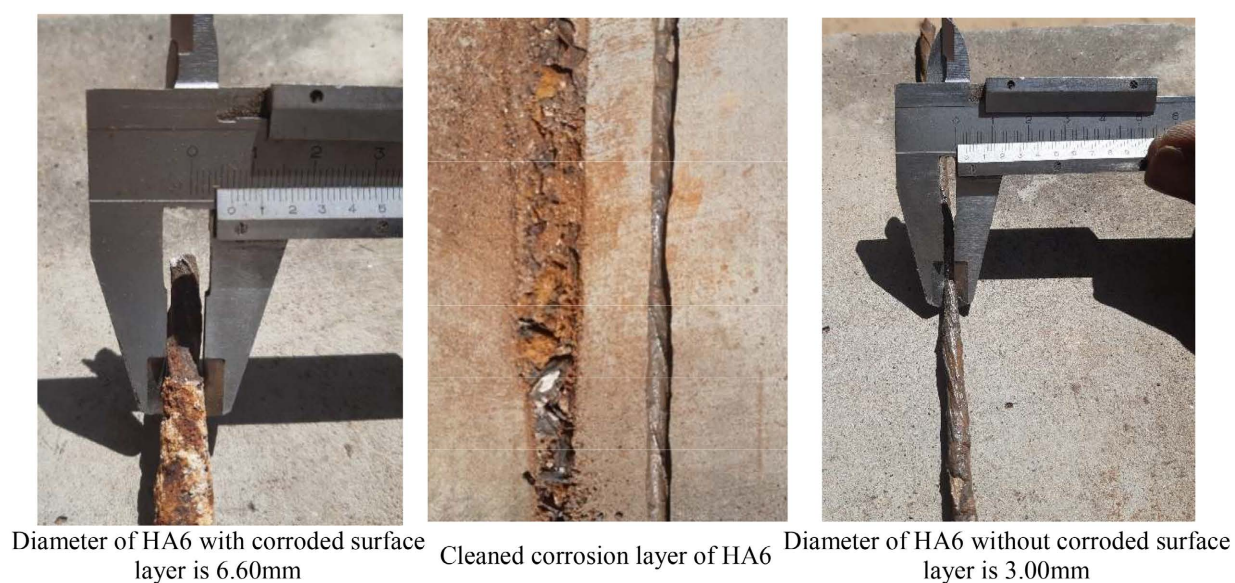


**Figure 4.** Operation to obtain the net section remaining after the corrosion of HA6.

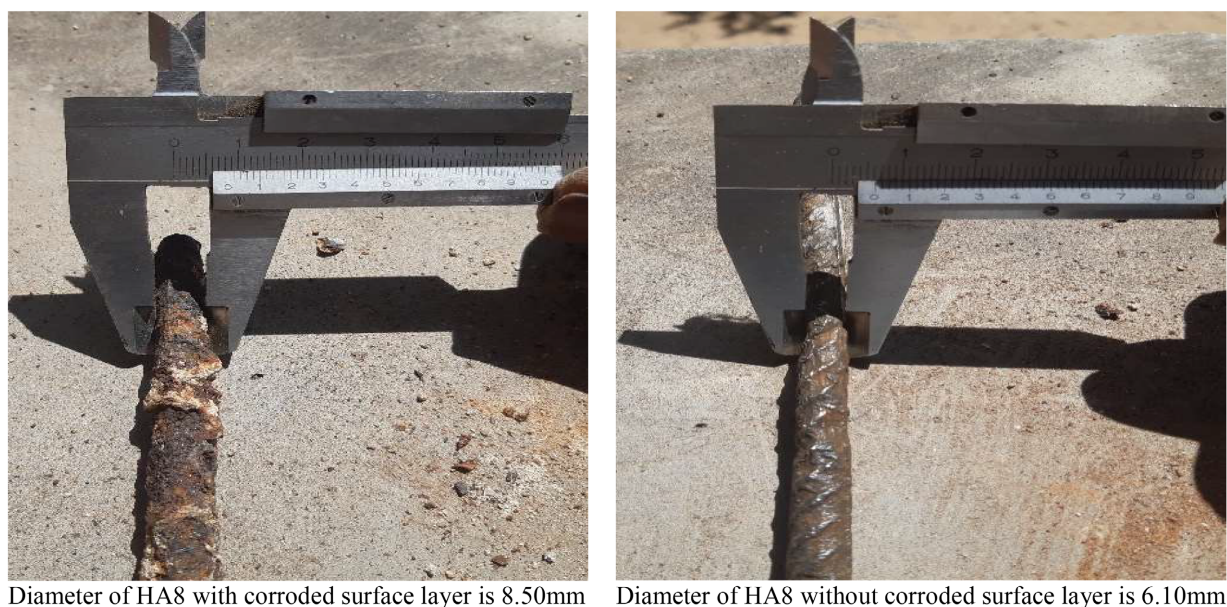


**Figure 5.** Operation to obtain the net section remaining after the corrosion of HA8.

5) Calculation of the corrosion rate ( $T_c$ )

It is defined by the following formula [62]:

$$T_c = \frac{\varnothing_{nc} - \varnothing_c}{\varnothing_{nc}} \quad (9)$$

with,  $\varnothing_{nc}$  is the uncorroded diameter and  $\varnothing_c$  is the corroded diameter

## 6) Modelling of degradation

Wagner's theory of oxidation kinetics (Equation 10) was used to model the progression of the corrosion layer over time (Figure 7). Considering the constant  $k = 0.2$ , we could theoretically plot the Wagner function under Matlab.

$$Y = k \cdot \sqrt{t} \quad (10)$$

with,  $Y$ : oxide thickness in  $\mu\text{m}$ ;  $t$  time in s and  $k$ : kinetic constant in  $\mu\text{m}/\text{s}^{1/2}$ .

The oxide curve progresses and stabilizes after a while, limited by an asymptote

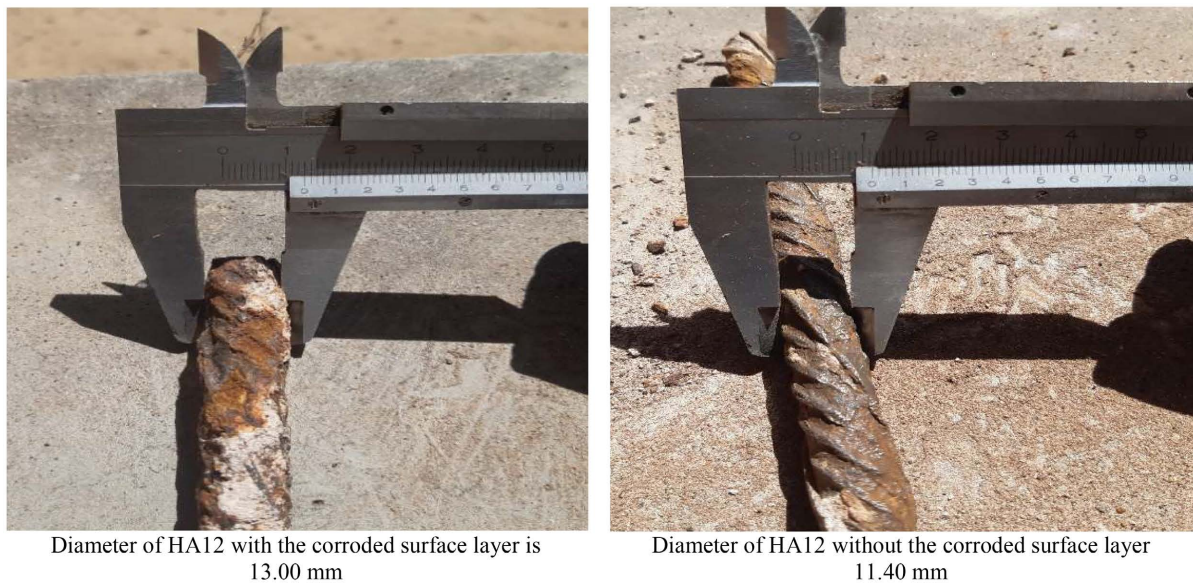


Figure 6. Operation to obtain the net section remaining after the corrosion of HA12.

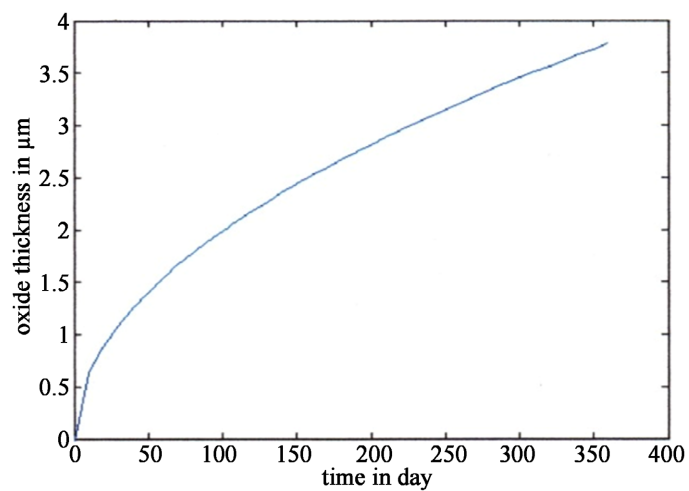


Figure 7. Progression of the corrosion layer.

defined by the maximum thickness. This is because the oxide layer behaves after a while, like a shield for steel.

## 4. Results and Discussion

### 4.1. Corrosion Rate ( $T_c$ )

The results of **Table 4** show that the corrosion rate is higher when the diameter of the reinforcements decreases. This fact influences the progression of the corrosion layer over time of Wagner's theory of oxidation kinetics which was used to model corrosion degradation (**Figure 7**). Indeed, this study shows through experimentation that two reinforcements of different diameters  $\varnothing_1 < \varnothing_2$  made of high-adhesion steel used in the same environmental conditions and stresses do not degrade in the same way by corrosion. The difference between the uncorroded diameter and the corroded diameter which represents the thickness of oxides in  $\mu\text{m}$  at a given time  $t$  varies depending on the diameter of the reinforcement. It is more important for  $\varnothing_1$  than for  $\varnothing_2$ . In **Figure 7**, we should plot the progression curves of the corrosion layer by diameter of reinforcement so that the curve C1 for the diameter  $\varnothing_1$  is greater than the curve C2 for the diameter  $\varnothing_2$ . In addition, as the rate of degradation is an inversely proportional function of the uncorroded diameter, it is quite justified that the rate of corrosion of  $\varnothing_1$  is higher than that of  $\varnothing_2$ .

Through this reality, we can safely accept that Wagner's model fits well with the experimental results of our study and as an example, consider the following application to show its interest.

A theoretical section of HA steel reinforcement for the reinforcement of a structural element has been calculated and is equal to  $A_{sth} = 1.08 \text{ cm}^2$ . Compared to the choice of reinforcements to reinforce this element, we have four possibilities: 4HA6 which gives a section of  $1.13 \text{ cm}^2$ ; 3HA8 -  $1.51 \text{ cm}^2$ ; 2HA10 -  $1.57 \text{ cm}^2$  and 1HA12 -  $1.13 \text{ cm}^2$ . Considering the unit prices of reinforcements in the city of N'Djamena for example, 1HA6 costs 1500 Fcfa, 1HA8 - 3500 Fcfa; 1HA10 - 4500 Fcfa and 1HA12 - 6500 Fcfa, the economical choice of a real section of Acre reinforcement  $\geq A_{sth} = 1.08 \text{ cm}^2$  will be made between 4HA6 and 1HA12 for which the real section is  $1.13 \text{ cm}^2$ . The untrained designer will simply choose 4HA6 to the detriment of an HA12. However, the corrosion rate of an HA12 is low compared to that of an HA6. This example of an RC choice of the real section of reinforcement often made by some designers is a shame for a structural element because according to the previous revelations, a reinforcement of

**Table 4.** Average values of the corrosion rates of the samples taken.

Sample	$\varnothing_{nc}$ (mm)	$\varnothing_c$ (mm)	$T_c$ (%)
HA6	6.00	3.00	50.00
HA8	8.00	6.10	23.75
HA12	12.00	11.40	5.00

large diameter corrodes less quickly than that of small diameter, and in more, according to paragraph 4.2, a low corrosion rate is synonymous with a less important loss of the tensile strength of the steel.

#### 4.2. Study of the Response of a Corroded Structural Element under Mechanical Loading

A simplified approach to the bearing capacity of structural elements (including HA10 steel reinforcements) as a function of the progress of the corrosion phenomenon was proposed by Mangat and Elgalf and will serve as an RCsis for interpreting the results of our work [63]. Steel admits the constitutive law proposed by Ouglova, which accounts for embrittlement due to corrosion [64]. The loss of steel section has been explicitly taken into account. Swelling could not be considered in this study, although it was essential to assess its impact on the initiation and propagation of cracks in concrete. The results presented in **Figure 8**, specific to Mangat and Elgalf, will be used to assess the behavioural impacts of degradation by corrosion of the HA steel reinforcements that we have sampled and studied. This proposed approach makes it possible to satisfactorily estimate the bearing capacity according to the corrosion level of samples such as those of Almussalam *et al.* 1996; Castel, 2001, etc.

We are aware that in an RC structure, the load-bearing capacity is generally relative to a load-bearing element of the structure such as column, beam, etc. and essentially depends on the ultimate strengths of the two components steel and concrete. Considering the assumption of the BAEL 91 mod.99 recalled in sub-paragraph 3.1.1, according to which the tensile strength of concrete is negligible, therefore, the bearing capacity of an element subjected to tensile or bending stresses will depend only on the steel, therefore of its ultimate resistance. This is why we use the diagram of Effort (in N)-Deflection (in mm) of the steel

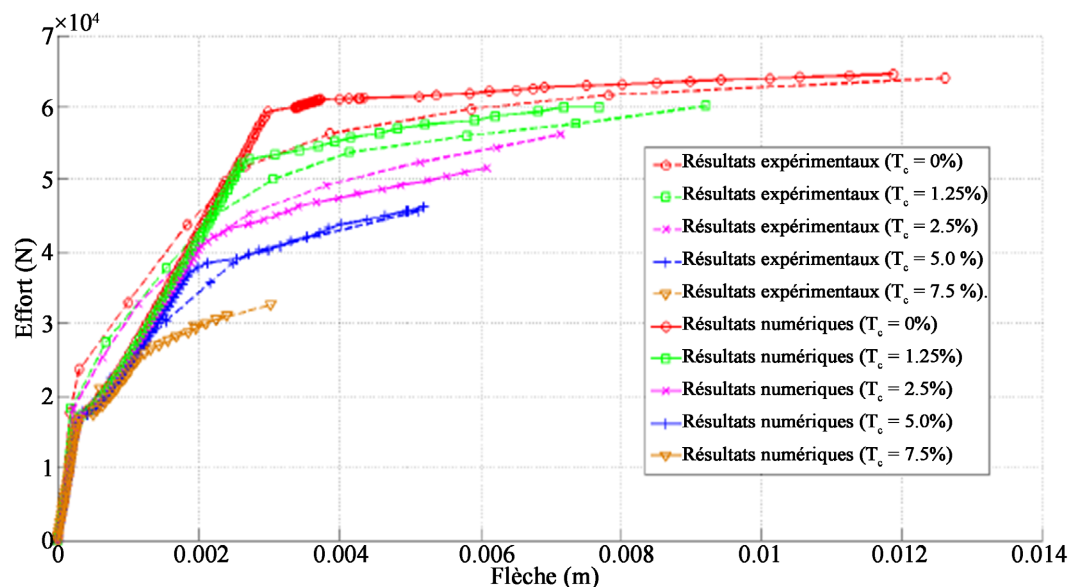


**Figure 8.** Results obtained for the beams tested by (Mangat and Elgalf, 1999)—simplified approach.

(Figure 8) to designate the bearing capacity or ultimate resistance to breaking or even ultimate resistance of an element structural feature mentioned in this study.

#### 4.2.1. HA6 Steel Reinforcement Sample

Sample HA6 is a 30 cm section of high-tack steel 6mm in diameter (Figure 2) which has been corroded (Figure 3). The entire rust layer was removed and the new diameter of the most degraded part could be measured with a calliper (Figure 4). The value read is 3 mm. Formula (9) above made it possible to calculate a corrosion rate of 50% reported in Table 4.

In Figure 8 established by Mangat and Elgalf, which gives the different behavioural curves of HA10 steels with various experimental and numerical corrosion rates, we notice that for a corrosion rate of 7.5%, the load-carrying capacity at break dropped by half (1/2) for a deflection of about 3 mm. This implies that for a corrosion rate of 50% determined on the HA6, the ultimate limit can be assumed to be negligible (*i.e.* the loss of the initial bearing capacity of the steel is considered equal to 100%, *i.e.* 4/4 of the initial ultimate resistance). Therefore, a column or beam having reinforcement with such a corrosion rate runs a great risk of bending failure.

#### 4.2.2. HA8 Steel Reinforcement Sample

Applying the same reasoning for the HA6 steel reinforcement sample and considering a corrosion rate for the HA8 sample (Figure 5) equal to 23.75%, the ultimate strength of this steel will decrease significantly by at most  $\frac{3}{4}$  of its initial ultimate strength with even higher risks of rupture for the reinforcements and therefore for the reinforced concrete.

#### 4.2.3. HA12 Steel Reinforcement Sample

Applying the same reasoning for the third HA12 sample (Figure 6) with a corrosion rate of 5%, the ultimate strength of this corroded steel will decrease by at most 1/4 of its initial ultimate strength.

By a logarithmic regression of the data RC on the results of this study, the trend curve of the loss of the bearing capacity as a function of the corrosion rate is presented in Figure 9. Above 50% corrosion rate, we can consider that the steel reinforcements no longer contribute to the resistance of an element of the structure. It emerges from this work that the corrosion rate of reinforcement is low when its nominal diameter is large and that the loss of the bearing capacity of a structural element is important when the corrosion rate is high.

Thus, the mathematical model of the loss of bearing capacity as a function of the corrosion rate can be written as below (11):

$$Y = 0.3013 \ln(x) + 1.2063 \quad (11)$$

with,  $Y$ : the loss of bearing capacity as a fraction of the initial ultimate strength of the steel considered;  $\ln$ : Natural logarithm and  $x$ : the corrosion rate in%.

Note that the coefficient of determination  $R^2 = 0.9714$  is close to 1.

In short, the loss of the bearing capacity of a structural member is an increasing

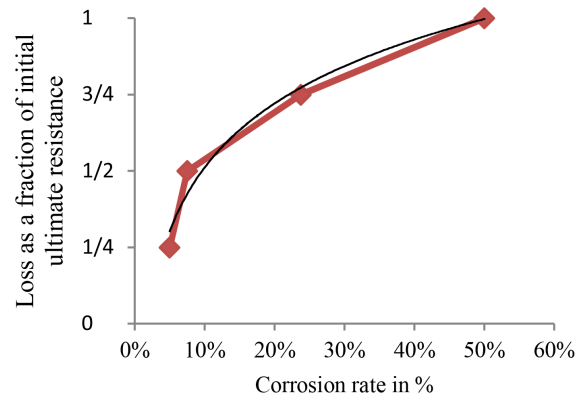


**Figure 9.** Trend curve for loss of bearing.

function of the rate of corrosion degradation. However, the study also shows that corrosion degradation rates are high for small reinforcement diameters. So, to guarantee a long-lasting life for a reinforced concrete structure, this study shows that we must avoid the excessive use of small diameter reinforcements. Also, this study shows that for a rational and durable operation of a complex steel-concrete element, it is not only necessary to avoid the corrosion of the steel in the concrete but it is also necessary an irreproachable adhesion allowing a good transmission of forces between concrete and steel.

Finally, at a given moment in the state of corrosion of the reinforcements in the concrete, when the tensile or bending stresses are greater than the bearing capacity or design limit resistance of an element of the structure, the cracks appears and the rupture is evident.

#### 4.2.4. Limitation of the Experimental Study

According to the diagram of **Figure 1**, we want to specify that the present study relates exclusively to the loss of the steel section at the local level by corrosion to estimate the reduction in the bearing capacity at the general level. To this end, the studies of the degradation of the interface by corrosion (cause of the loss of adhesion) and of the volumetric expansion by corrosion (cause of the disappearance of the ribs) which was briefly approached and which was not developed during this experiment is the subject of studies in perspective.

During the experiment, we found that at any given time  $t$ , the progression of the corrosion layer varied depending on the diameters of the reinforcement samples tested. Normally, according to our understanding, two reinforcements of different diameters made of the same high adhesion material, used under the same environmental and stress conditions must corrode in the same way therefore have an equal thickness of the corrosion layer. We were unable to identify this contradiction and believe that this is certainly due to the multitude and complexity of certain causes of corrosion announced in paragraph 2.2.

## 5. Conclusions

We have focused this work on part of the effects of degradation phenomena of

the steel-concrete interfaces which, it should be remembered, are physical and chemical. The experimental work was exclusively carried out on the consequences of chemical degradation by the corrosion of steel in concrete. To this end, it was first necessary to recall the degradation phenomena of the loss of adhesion between steel and concrete and the phenomenon of corrosion of steel in concrete. The second step is to notify the composition of this interface by defining the components that are concrete and steel with their different properties to highlight any incompatibility problem between these two materials. The essential concepts related to the behaviour of the steel-concrete interface were also discussed. Subsequently, it was ultimately on chemical degradation, namely corrosion by loss of steel section, that work was carried out to assess their impact on the weakening of reinforced concrete structures.

Thus, several samples were taken of corroded high adhesion steels with initial diameters HA6, HA8 and HA12. The layers of rust were carefully removed and the deeply cut diameters were measured. After calculating the corrosion degradation rate, this work reveals two important pieces of information:

- From experience, the smaller the nominal diameter of the steel reinforcement, the higher the corrosion rate.
- RC on the work of Mangat and Elgalf, we can say that the higher the corrosion rate of HA steel reinforcement, the greater the loss of its ultimate limit.

### Conflicts of Interest

The authors declare no conflicts of interest regarding the publication of this paper.

### References

- [1] Lutz, L.A. and Gergely, P (1967) Mechanism of Bond and Slip of Deformed Bars in Concrete. *ACI Journal Proceedings*, **64**, 711-721. <https://doi.org/10.14359/7600>
- [2] Dahou, Z., Sbartai, Z.M., Castel, A. and Ghomari, F. (2009) Artificial Neural Network Model for Steel-Concrete Bond Prediction. *Engineering Structures*, **31**, 1724-1733. <https://doi.org/10.1016/j.engstruct.2009.02.010>
- [3] Daoud, A. (2003) Etude expérimentale de la liaison entre l'acier et le béton auto plaçant—Contribution à la modélisation numérique de l'interface. Mémoire de Thèse, Institut National des Sciences Appliquées de Toulouse, Toulouse, 194.
- [4] Daoud, A., Maurel, O. and La Borderie, C. (2013) Modélisation de l'interface acier-béton par une approche mésoscopique. *Engineering Structures*, **49**, 696-706. <https://doi.org/10.1016/j.engstruct.2012.11.018>
- [5] Desnerck, P., De Schutter, G. and Taerwe, L. (2010) Bond Behaviour of Reinforcing Bars in Self-Compacting Concrete: Experimental Determination by Using Beam Tests. *Materials and Structures*, **43**, 53-62. <https://doi.org/10.1617/s11527-010-9596-6>
- [6] Dominguez, N. (2005) Etude de la liaison acier-béton: De la modélisation de phénomène à la formulation d'un élément fini enrichi "béton armé". Mémoire de Thèse, Ecole Normale Supérieure de Cachan, Cachan.
- [7] Eligehausen, R., Popov, E. and Bertero, V. (1983) Local Bond Stress-Slip Relation-

- ships of Deformed Bars under Generalized Excitations: Experimental Results and Analytical Model. Report, Earthquake Engineering Research Center, College of Engineering, University of California, Oakland, CA.
- [8] Esfahani, M., Lachemi, M. and Kianoush, M. (2008) Top-Bar Effect of Steel Bars in Self-Consolidating Concrete (SCC). *Cement and Concrete Composite*, **30**, 52-60. <https://doi.org/10.1016/j.cemconcomp.2007.05.012>
- [9] Eurocode 2-1-1 (2005) Eurocode 2: Calcul des structures en béton, Partie 1-1: Règles générales et règles pour les bâtiments.
- [10] Frederick, C.O. and Armstrong, P. (2007) A Mathematical Representation of the Multiaxial Bauschinger Effect. *Materials at High Temperatures*, **24**, 1-26.
- [11] Gambarova, P.G. and Rosati, G. (1996) Bond and Splitting in Reinforced Concrete: Test Results on Bar Pull-Out. *Materials and Structures*, **29**, 267-276. <https://doi.org/10.1007/BF02486361>
- [12] Ngo, D. and Scordelis, A. (1967) Finite Element Analysis of Reinforced Concrete Beams. *ACI Journal Proceedings*, **64**, 152-163. <https://doi.org/10.14359/7551>
- [13] Ouglova, A. (1999) Etude du comportement mécanique des structures en béton armé atteintes par la corrosion. Mémoire de Thèse, Ecole Normale Supérieure de Cachan, Cachan.
- [14] Phan, T., Tailhan, J.-L., Rossi, P., Bressolette, P. and Mezghani, F. (2013) Numerical Modelling of the Rebar/Concrete Interface: Case of the Flat Steel Rebars. *Materials and Structures*, **46**, 1011-1025. <https://doi.org/10.1617/s11527-012-9950-y>
- [15] Mezhoud, D., *et al.* (2017) Etude expérimentale de l'adhérence acier-béton à l'aide de la technique d'émission acoustique. *AJCE-Spécial Issue*, **35**, 759-762.
- [16] (1970) Essais portant sur l'adhérence des armatures du béton: 2: Essai par traction. *Materials and Structures*, **3**, 175-178. <https://doi.org/10.1007/BF02478968>
- [17] Ragueneau, F. (1999) Fonctionnement dynamique des structures en béton—Influence des comportements hystérétiques locaux. Mémoire de Thèse, Ecole Normale Supérieure de Cachan, Cachan.
- [18] Ragueneau, F., Dominguez, N. and Ibrahimbegovic, A. (2006) Thermodynamic-Based Interface Model for Cohesive Brittle Materials: Application to Bond Slips in RC Structures. *Computer Methods in Applied Mechanics and Engineering*, **195**, 7249-7263. <https://doi.org/10.1016/j.cma.2005.04.022>
- [19] Ragueneau, F., Richard, B., Crémona, C. and Berthaud, Y. (2010) Damage Mechanics Applied to the Modelling of Corroded Reinforced Concrete Structures: Steel, Concrete and Interface. *European Journal of Environmental and Civil Engineering*, **14**, 869-890. <https://doi.org/10.1080/19648189.2010.9693267>
- [20] Mikael, D. (2003) Etude du comportement mécanique des structures en béton armé dégradé par la corrosion. Thèse de Doctorat, Université de Lille 1, Lille.
- [21] Rehm, G. and Van Amerongen, C. (1968) The Basic Principles of the Bond between Steel and Concrete. Cement and Concrete Association.
- [22] Richard, B., Ragueneau, F., Cremona, C. and Adelaide, L. (2010) Isotropic Continuum Damage Mechanics for Concrete under Cyclic Loading: Stiffness Recovery, Inelastic Strains and Frictional Sliding. *Engineering Fracture Mechanics*, **77**, 1203-1223. <https://doi.org/10.1016/j.engfracmech.2010.02.010>
- [23] Richard, B., Ragueneau, F., Cremona, C., Adelaide, L. and Tailhan, F. (2010) A Three-Dimensionnal Steel/Concrete Interface Model Including Corrosion Effects. *Engineering Fracture Mechanics*, **77**, 951-973. <https://doi.org/10.1016/j.engfracmech.2010.01.017>

- [24] Rousseau, J. (2009) Modélisation numérique du comportement dynamique de structures sous impact sévère avec un couplage éléments discrets/éléments finis. Mémoire de Thèse, Université Joseph Fourier, Grenoble.
- [25] Huet, B. (2005) Comportement à la corrosion des armatures dans un béton carbonaté: Influence de la chimie de la solution interstitielle et d'une barrière de transport. Thèse de Doctorat Unique des Universités, Institut National des Sciences Appliquées (INSA) de Lyon.
- [26] Mai-Nhu, J. (2013) Corrosion des armatures du béton couplage carbonatation/chlorures en présence de cycles hydriques. Thèse de Doctorat de l'Université de Toulouse, France.
- [27] Zhang, L. and Glasser, F.P. (2005) Investigation of the Microstructure and Carbonation of CS<sup>-</sup>A-Based Concretes Removed from Services. *Cement and Concrete Research*, **35**, 2252-2260. <https://doi.org/10.1016/j.cemconres.2004.08.007>
- [28] Paradis, F. (2009) Influence de la fissuration du béton sur la corrosion des armatures: Caractérisation des produits de la corrosion formés dans le béton. Thèse de Doctorat de l'Université de Laval, Canada.
- [29] Loukil, O. (2017) Etude expérimentale et numérique de la dégradation d'éléments structurels en béton armé par corrosion sous courant imposé. Thèse de Doctorat. <http://tel.archives-ouvertes.fr>
- [30] Wang, L., Yi, J., Xia, H.L. and Fan, L. (2016) Experimental Study of a Pull-Out Test of Corroded Steel and Concrete Using the Acoustic Emission Monitoring Method. *Construction and Building Materials*, **122**, 163-170. <https://doi.org/10.1016/j.conbuildmat.2016.06.046>
- [31] Maslehudin, M., Al-Zahrani, M.M. and Al-Dulaijan, S.U. (2002) Effect of Steel Manufacturing Process and Atmospheric Corrosion on the Corrosion-Resistance of Steel Bars in Concrete. *Cement and Concrete Composites*, **24**, 151-158. [https://doi.org/10.1016/S0958-9465\(01\)00035-X](https://doi.org/10.1016/S0958-9465(01)00035-X)
- [32] Avila-Mendoza, J., Flores, J.M. and Castillo, U.C. (1994) Effect of Superficial Oxides On corrosion of Steel Reinforcement Embedded in Concrete. *Corrosion*, **50**, 879-885. <https://doi.org/10.5006/1.3293478>
- [33] Gonzalez, J.A. (1996) The Behaviour of Pre-Rusted Steel in Concrete. *Cement and Concrete Research*, **26**, 501-511. [https://doi.org/10.1016/S0008-8846\(96\)85037-X](https://doi.org/10.1016/S0008-8846(96)85037-X)
- [34] Novak, P., Mala, R. and Joska, L. (2001) Influence of Pre-Rusting on Steel Corrosion in Concrete. *Cement and Concrete Research*, **31**, 589-593. [https://doi.org/10.1016/S0008-8846\(01\)00459-8](https://doi.org/10.1016/S0008-8846(01)00459-8)
- [35] Page, C.L. (1975) Mechanism of Corrosion Protection in Reinforced Concrete Marine Structures. *Nature*, **258**, 514-515. <https://doi.org/10.1038/258514a0>
- [36] Glass, G.K., Yang, R. and Dickhaus, T. (2001) Backscattered Electron Imaging of the Steel Concrete Interface. *Corrosion Science*, **43**, 605-610. [https://doi.org/10.1016/S0010-938X\(00\)00146-3](https://doi.org/10.1016/S0010-938X(00)00146-3)
- [37] Trujillo, P.B., Jolin, M. and Massicotte, B. (2012) Défauts à l'interface barre d'armature-béton et leur influence sur l'adhérence.
- [38] Mouats, M. (2013) Caractérisation mécanique des éléments corrodés en béton armé, cas d'un béton ordinaire. Mémoire en vue de l'obtention du diplôme de Master en Génie civil 2013-Université Mentori Constantine.
- [39] Jean, P.M. Béton armé. BAEL 91 modifiées 99 et DTU associés, Edition Eyrolles.
- [40] Cains, J. and Millard, S. (1999) Reinforcement Corrosion and Its Effect on Residual Strength of Concrete Structure. *Proceedings of the 8th International Conference on*

*Structural Faults and Repair*, London, 1 January 1999, 1-12.

- [41] NPL (2003) A Short Introduction to Corrosion and Its Control, Corrosion in the Metals and Its Prevention. National Corrosion Service.
- [42] Mehibil, R. (2010) Etude de l'efficacité inhibitrice de quelques nouveaux inhibiteurs, dits non polluants, sur la corrosion de deux types d'alliages d'aluminium. Université de Skikda, Skikda.
- [43] Tixier, A. (2013) Analyse du comportement de l'interface acier-béton par essai push-in: Mesure par fibre optique et modélisation par éléments finis. Thèse de Doctorat de l'Université de Grenoble, France.
- [44] CEB-FIP (1982) Design of Concrete Structures for Fire Resistance. Model code.
- [45] CEB-FIB (1993) Model Code 1990. Design Code. Rapport Technique, Comité Euro-International du Béton.
- [46] Clément, J. (1987) Interface acier-béton et comportement des structures en béton armé: Caractérisation et modélisation. Mémoire de Thèse, Université de Paris VI, Paris.
- [47] Gambarova, P.G. and Rosati, G.P. (1997) Bond and Splitting in Bar Pull-Out: Behavioural Laws and Concrete Cover Role. *Magazine of Concrete Research*, **49**, 99-110. <https://doi.org/10.1680/mac.1997.49.179.99>
- [48] Michel-Ponnelle, S., Joint-RC (2005) Loi de comportement (en 2D) dans Code\_Aster pour la liaison acier-béton. [http://www.code-aster.org/V2/doc/v9/fr/man\\_r/r7/r7.01.21.pdf](http://www.code-aster.org/V2/doc/v9/fr/man_r/r7/r7.01.21.pdf)
- [49] Klinkenberg, L. (1941) The Permeability of Porous Media to Liquids and Gases, American Petroleum Institute. In: *Drilling and Production Practice*, 200-213.
- [50] La Borderie, C. and Pijaudier-Cabot, G. (1992) Influence of the State of Stress in Concrete on the Behavior of the Steel Concrete Interface. In: Bazant, Z.P., Ed., *Fracture Mechanics of Concrete Structures*, CRC Press, London.
- [51] Perchat, J. (2010) Traité de béton armé. Des règles RCEL à l'Eurocode 2, Edition du Moniteur.
- [52] Tepfers, R. (1979) Cracking of Concrete Cover along Anchored Deformed Reinforcing Bars. *Magazine of Concrete Research*, **31**, 3-12. <https://doi.org/10.1680/mac.1979.31.106.3>
- [53] Tilantera, T. and Rechart T. (1977) Bond of Reinforcement in Light-Weight Aggregate Concrete. Otanjemi, Helsinki University of Technology, Division of Structural Engineering, Publication 17, 1-36.
- [54] Damien, R. (1992) Dimensionnement des structures en béton selon Eurocode 2, Editions du Moniteur.
- [55] Karavokyros, L., Batis, G., Katsiotis, N., Tzani, E. and Beazi-Katsioti, M. (2020) Durability of Reinforced Concrete Beams under Simultaneous Flexural Load in Corrosive Environment. *Journal of Materials Science and Chemical Engineering*, **8**, 32-45. <https://doi.org/10.4236/msce.2020.84003>
- [56] Ouglova, A., Berthaud, Y., Foct, F., François, M., Ragueneau, F. and Petre-Lazar, I. (2008) The Influence of Corrosion on Bond Properties between Concrete and Reinforcement in Concrete Structures. *Materials and Structures*, **41**, 969-980. <https://doi.org/10.1617/s11527-007-9298-x>
- [57] Cao, C., Cheung, M.M. and Chan, B.Y. (2013) Modelling of Interaction between Corrosion-Induced Concrete Cover Crack and Steel Corrosion Rate. *Corrosion Science*, **69**, 97-109. <https://doi.org/10.1016/j.corsci.2012.11.028>
- [58] Zhang, F., Pan, J.S. and Lin, C.J. (2009) Localized Corrosion Behaviour of Rein-

- forcement Steel in Simulated Concrete Pore Solution. *Corrosion Science*, **51**, 2130-2138. <https://doi.org/10.1016/j.corsci.2009.05.044>
- [59] Alvarez, S., Bautista, A. and Velasco, F. (2011) Corrosion Behaviour of Corrugated Lean Duplex Stainless Steels in Simulated Concrete Pore Solutions. *Corrosion Science*, **53**, 1748-1755. <https://doi.org/10.1016/j.corsci.2011.01.050>
- [60] Shi, J.J., Sun, W., Jiang, J.Y. and Zhang, Y.M. (2016) Influence of Chloride Concentration and Pre-Passivation on the Pitting Corrosion Resistance of Low-Alloy Reinforcing Steel in Simulated Concrete Pore Solution. *Construction and Building Materials*, **111**, 805-813. <https://doi.org/10.1016/j.conbuildmat.2016.02.107>
- [61] Hariche, L., Ballim, Y., Bouhicha, M. and Kenai, S. (2012) Effects of Reinforcement Configuration and Sustained Load on the Behaviour of Reinforced Concrete Beams Affected by Reinforcing Steel Corrosion. *Cement and Concrete Composites*, **34**, 1202-1209. <https://doi.org/10.1016/j.cemconcomp.2012.07.010>
- [62] Feng, X.G., Tang, Y.M. and Zuo, Y. (2011) Influence of Stress on Passive Behaviour of Steel Bars in Concrete Pore Solution. *Corrosion Science*, **53**, 1304-1311. <https://doi.org/10.1016/j.corsci.2010.12.030>
- [63] Wang, H.L., Lu, C.H., Jin, W.L. and Bai, Y. (2011) Effect of External Loads on Chloride Transport in Concrete. *Journal of Materials in Civil Engineering*, **23**, 1043-1049. [https://doi.org/10.1061/\(ASCE\)MT.1943-5533.0000265](https://doi.org/10.1061/(ASCE)MT.1943-5533.0000265)
- [64] Jaffer, S. and Hansson, C. (2008) The Influence of Cracks on Chloride-Induced Corrosion of Steel in Ordinary Portland Cement and High Performance Concretes Subjected to Different Loading Conditions. *Corrosion Science*, **50**, 3343-3355. <https://doi.org/10.1016/j.corsci.2008.09.018>